A 5 ton demonstrator for large-scale dual phase liquid argon time projection chambers

Abstract

Keywords: Neutrino, liquid argon TPC

Contents

1 Introduction 2

2 Overview of the set-up 4

3 Cryostat and cryogenic system 5
- 3.1 The cryostat . . . 7
- 3.2 The cryogenic and argon purification system . . . 9
  - 3.2.1 Gas argon piston purge, cooling down and filling . . . 10
  - 3.2.2 Boil off compensation and liquid purification during detector operation 12
- 3.3 Cryostat and cryogenic system performance . . . 12

4 Description of the TPC 14
- 4.1 Drift cage, cathode and high voltage feedthroughs . . . 14
- 4.2 Charge readout plane . . . 15
  - 4.2.1 Mechanical frame and suspension system . . . 15
  - 4.2.2 Large Area LEMs and anodes . . . 15
  - 4.2.3 LEM biasing and medium voltage feedthroughs . . . 15
- 4.3 Photon detection system . . . 17

5 Charge Readout scheme and data processing 18
- 5.1 Cold analog Front Ends and signal feedthrough . . . 18
- 5.2 Front Ends cards and ASIC characteristics . . . 18
- 5.3 Digital back end and data acquisition . . . 18

6 Ancillary instrumentation and slow control 18
- 6.1 level monitoring and feedback to charge readout plane suspension . . . 18
- 6.2 Cryogenic cameras . . . 18
- 6.3 Slow control back-end . . . 20

Preprint submitted to NIM *November 30, 2017*

7 Dector commissioning and first data 20
7.1 Stability of liquid level and charge readout plane adjustment 20
7.2 high voltage system settings and stability 20
7.3 Charge readout performance and response 20
7.3.1 Electronic noise study 20
7.3.2 Response to an injected pulse 20
7.4 Photon detection system performance 20
7.5 First data 20
7.5.1 Electroluminescence and evidence for charge extraction 20
7.5.2 Observation of first cosmic muons with gain 20

1. Introduction

Liquid argon time projection chamber (LAr TPC) is the detector technology chosen for the DUNE (Deep Underground Neutrino Experiment) experiment [1]. DUNE is the next generation of underground experiments aiming to study neutrino properties from both man-made and natural sources as well as probe the grand unification energy scale via nucleon decay searches. Such varied program requires a massive detector with active volume on a multi-kt scale. Numerous R&D efforts throughout the world have been aimed at realizing this goal. In Europe, a solution has been developed within the LAGUNA-LBNO design study for a LAr TPC detector with a mass of 20 kt to 50 kt [2]. The detector concept relies on the amplification of ionisation charges in ultra-pure cold argon vapour layer above the liquid to realize low-energy detection thresholds with high signal-to-noise (S/N) ratio over a long drift distances in a large fully-active volume.

The principle of operation of the LAr TPC relies on the detection of ionisation electrons — produced in the liquid argon by charged particles traversing the medium — on sets of electrodes that provide the two-dimensional localisation of the point where the energy deposition had occurred. The time it takes for the charge cloud to arrive at the electrodes under influence of an electric (drift) field inside active TPC volume gives the third spatial coordinate along the axis parallel to the drift direction. In addition to charge, ionising particles produce excited excimer states of Ar that decay by emitting photons in ultraviolet range (128 nm). This light, recorded with a suitable cryogenic photon-detection system, provides an absolute time reference for the event with respect to a global clock cycle and could be used to trigger charge readout electronics.

Traditionally the ionisation charge in LAr TPC has been detected inside liquid volume using a set of wire planes (views). Typically three views are used with the first two (in the sense encountered by the drifting electrons) detecting electrons by induction while the third and the last one collects the charges. In the case of the LAr TPC with dual-phase charge readout (DLAr TPC), the ionisation electrons are drifted upwards to the gas-liquid boundary and then extracted into gaseous phase with a help of submerged grid of wires that provide a local field of ~ 2 kV/cm. Once in the gas, electrons are multiplied in Townsend avalanches taking place in the holes of a 1 mm thick GEM or LEM (Large Electron Amplifier) [3]. The resultant charge is collected on an anode with a two-dimensional segmentation providing two orthogonal detection views. The structure of the extraction grid, LEM, and anode will collectively be referred to as Charge Readout Plane (CRP) in the rest of the paper.

The amplification of charge (or gain) in the dual-phase readout scheme allows to cope with a weakening of the signal strength due to electron attachment to electronegative impurities in liquid Argon and diffusion effects thereby making it possible to build large detector volumes with long drift distances. The gain factor could be tuned by adjusting the electric field strength in the LEM to achieve a good S/N ratio with a fine readout pitch of ~ 3 mm. In addition, the anode provides two symmetric collection strips, removing any induction views which are more problematic to read out and reconstruct. The fact that the anode plane is located in the gas also makes it insensitive to any possible microphonic pick-up noise generated inside the liquid volume. The charge amplification and readout in pure argon vapour has been a subject of an extensive R&D in the last decade. Detectors varying in scales from 3L to 250L volume have been built and successfully operated over significant periods of time [4, 5]. In recent years developments have been targeted towards scaling up the system to meter squared readout areas [].

Construction and operation of a large-scale ~ 300 t ($6\times6\times6$ m^3 active volume) dual-phase LAr TPC is the ultimate goal of the WA105 experiment at CERN [6]. It is the key milestone towards deploying this detector technology on multi-kt scale. To prototype and test a number of critical sub-systems for the WA105 experiment a pilot technical demonstrator with an active TPC volume of $3 \times 1 \times 1$ m^3 has been developed. This detector is the subject of the paper. As a first ton-scale demonstrator of the dual phase LAr TPC we list below set of key technological deliverable and first operational milestones aiming to validate the technology and the progress achieved in this first step towards the construction of kton scale detectors.

i) Liquid argon purity at the $\leq$100 ppt level and stability of the liquid and gas argon thermodynamic conditions in a 23 m^3 non evacuable membrane cryostat. The construction and operation of the $3 \times 1 \times 1$ m^3 represents a unique test bed to understand some essential installation, operational and performance aspects to address the suitability of those types of cryostats for future large dual phase LAr TPCs. The cryogenic system, the argon re-circulation, purification and cooling methods will also be discussed.

ii) Extraction of the ionization charge and amplification in purge argon vapour over an area of 3 m^2. Never before has charge been extracted from liquid argon over such a large area. The concept of a charge readout plane mechanically and electronically independent from the main drift volume will be discussed. Its performance in terms of extraction efficiency and the details of the amplification devices will be described in detail.

iii) Readout of the signal on two collection planes with strips of up to 3 m length. performance of cold analogue front end electronics. An important aspects of the dual-phase TPC with its vertical drift is the ability to position front-end electronics closes to the readout strips while at the same time ensuring its accessibility during detector operation. The charge readout scheme will be described in detail

The manuscript is organized as follows. In Section 3 the overview of the cryostat and cryogenic system is provided. Section 4 describes the TPC and photon detection system in detail. The charge readout, the analog and digital electronics as well as the data processing is discussed in Section 5. The trigger, data acquisition, as well as the on-line storage and processing units is covered in Section **??**. Sections 6 will present the slow control system and some innovative type of instrumentation to monitor the conditions inside the cryostat. Finally, section 7 will show some initial results from the detector commissioning and operation.

2. Overview of the set-up

The experimental setup is illustrated in Figure 1. It consists of a $3 \times 1 \times 1$ m^3 active volume dual phase LAr-TPC inside a passively insulated cryostat with internal volume of $\sim$23 m^3. The TPC is composed of a one meter high field cage made by 19 field shapers placed at a constant spacing of 50 mm and a metallic grid cathode at the bottom. A uniform drift field is provided by a resistor divider chain situated between the cathode and the top field shaper. At the top of the drift cage the drifting charges are extracted to the gas phase where they are amplified and readout by a 3×1 m^2 charge readout plane (CRP). The CRP is a single frame electrically and mechanically independent from the drift cage that can be remotely adjusted to the liquid level with 100 micron precision by means of three suspension cables. It contains an extraction plane provided by a 3 mm pitch wire-mesh, an amplification plane made from individually powered 50 $\times$50 cm^2 LEMs of 1 mm thickness and a readout stage provided by 50 $\times$50 cm^2 printed circuit board anodes. The anodes are electrically bridged together to provide readout strips of 3 meter and 1 meter length. The CRP is designed to preserve a uniform 1 cm distance between the extraction-amplification plane (extraction gap) and a 2 mm distance between the amplification-readout plane (induction gap). In nominal operating conditions the liquid level is adjusted in the middle of the extraction gap, 5 mm above the wire-mesh. A detailed description of the CRP is provided in Section 4. Five photo-multiplier tubes (PMTs) coated with the wavelength shifter, TPB, are fixed to the bottom of the cryostat under a ground protecting grid. They are sensitive to the 128 nm scintillation light from the argon scintillation and provide the reference time for the drift as well as the trigger. The entire detector is hung under a 1.2 m thick insulating top cap. The field cage is fixed by eight FR4 bars and the CRP is suspended by the three adjustable cables inserted in dedicated motorised feedthroughs. The position of the CRP with respect to the LAr level is constantly readout by seven capactive level meters placed on the periphery of the CRP frame. The level meters have range of 25 mm and and accuracy of 100 microns which allow, together with the motorized suspension system, a precise alignment of the CRP to the level. The adjustment is performed once after the first filling of the cryostat and, unless of sudden changes in the level, the CRP remains locked at this set position during the entire data taking.

The top cap is part of the cryostat structure providing the functionality of reducing heat input and minimizing the liquid and gas Argon convection. The TPC is pre-assembled under the top-cap in a custom built clean room ”tent” and then inserted in the main cryostat as shown in Figure 3. Subsequent access inside the cryostat is performed through the top-cap via 600 mm diameter manhole. Temperature and level measurements.

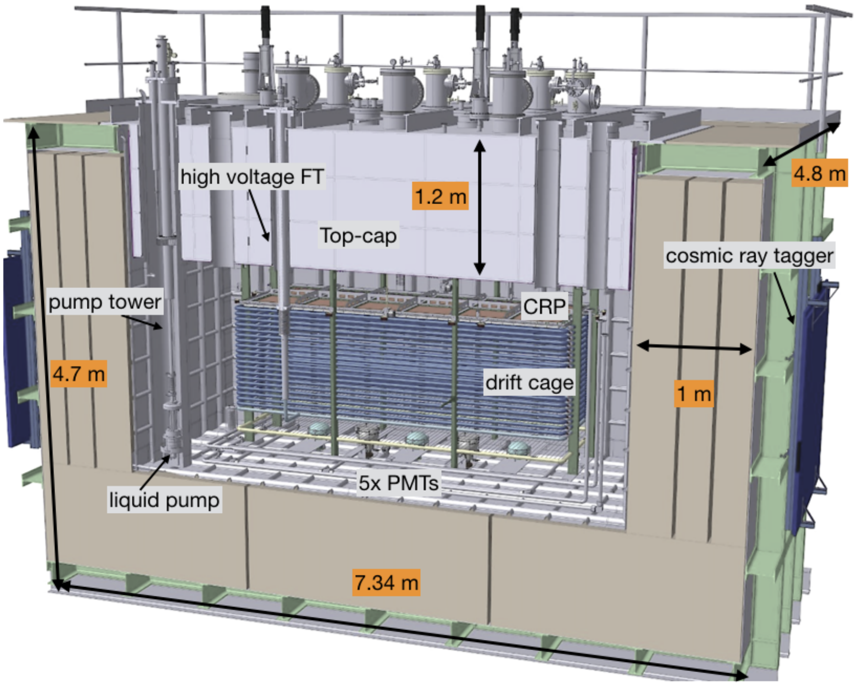

Figure 1: Drawing of the WA105-3 $\times$ 1 $\times$ 1 m^3 dual phase LAr TPC in the cryostat.

3. Cryostat and cryogenic system

The cryostat and the cryogenic system serve a multipurpose role that is critical to the good functioning of the dual phase TPC. The cryostat is operated as a totally sealed system near atmospheric pressure. The liquid argon is left to evaporate at a rate that depends on the insulation quality of the cryosat and on the total heat input provided to the system. The evaporated gas (the so called *boil-off*) and the liquid are constantly recirculated and purified in a closed loop. Some specifications of the cryostat and of the cryogenic system are provided in Table 1. The main operational quantities that depend upon the performance of the cryostat and cryogenic installation are listed below.

- *Gas argon density.* The thermodynamic properties of the gas argon need to be well controlled and measured since the gas density has an impact on the value of the amplification inside the LEM holes. The TPC is to be operated at a constant $P_{cryostat} \sim$ 1 Atm and a uniform gas temperature measured at the LEMs of around $\sim$ 90 K. With those settings previous dual phase TPCs were operated at stable gain of around 20 [7, 8] for long periods. In those chambers the pressure was either controlled or measured at the level of $\sim$1 mbar and the temperature was stable within one degree.

- *Liquid level.* The value of the extraction electric field in the liquid, ε_{extr}, is determined by the difference in potential over the 1 cm grid-LEM distance and the position of the LAr level in-between the two planes. It has been measured in the past [9] and more recently in smaller dual phase chambers [10?] that above $\varepsilon_{extr} > 2$ kV/cm the extraction efficiency is near 100%. Operating the detector at $\varepsilon_{extr} \simeq 3$ kV/cm thereby guarantees that close to 100% of the drifting charges are extracted from the liquid independently of fluctuations in the level. This is illustrated in Figure 2 where ε_{extr} is plotted as a function of the LAr level for various grid-LEM potential differences. Our requirements on the liquid level position are instead driven by the boundary conditions that on one hand the LEMs should not be immersed and on the other that the extraction grid must stay inside in the liquid. We therefore require that the CRP frame should be aligned with respect to the liquid level within 1-2 mm over its entire 3 m^2 surface and constantly monitored at the sub-mm scale. The cryogenic system is setup in such a way that it self-regulates to keep the absolute level inside the cryostat at a constant value. The global heat input from the cryostat and various sources should be compensated by the cooling system to maintain the LAr level relatively flat and avoid large waves on the surface. Local heat inputs that may also introduce undesired bubbling should be avoided for the same reason. The precise alignment of the CRP with respect to the liquid is discussed in Section 7

- *Liquid purity.* A constant liquid argon purity of better than 100 ppt oxygen equivalent, or similarly an electron lifetime of 3 ms, is required in order to efficiently transport the electrons over the $\mathcal{O}(10)$ meter drifts proposed in future large dual phase TPCs [11, 12]. This setup, although of more modest drift distance, offers a unique test bed to verify if the cryostat and the purification systems are capable of achieving and maintaining such purities over long periods.

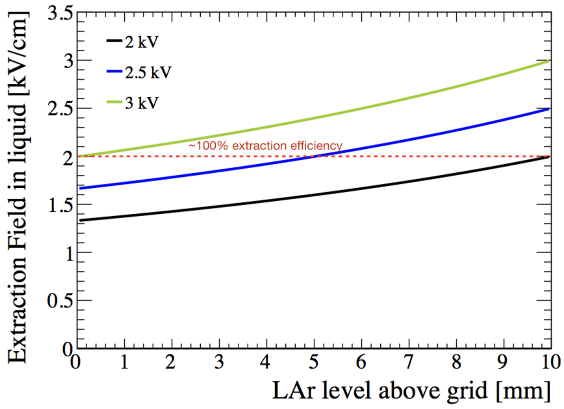

Figure 2: extraction field in the liquid as a function of the liquid argon level above the extraction grid for different voltages applied across the grid-LEM planes. The dotted red line indicates the electric field in liquid above which ∼100% of the charges are extracted according to Ref.[9]. FIXME maybe move this plot some place else.

	Component	value	unit
cryostat			
	outer dimensions (l×w×h)	$7.34 \times 4.88 \times 4.76$	m^3
	inner dimensions (l×w×h)	$4.76 \times 2.38 \times 2.03$	m^3
	main vessel (top cap) insulation thickness	1 (1.2)	m
	nominal volume of LAr (GAr)	18.01 (4.98)	m^3
	nominal height of LAr (GAr)	1590 (440)	mm
	designed pressure range	995-1090	mbar
	operating pressure	998	mbar
	GAr temperature gradient near the liquid	$\sim$2	K/cm
	GAr temperature extrapolated to LEM	95	K
liquid purification			
	pump model	ACD-TC34.2	
	pump nominal (max) flow rate	22 (35)	lpm
	cartridge active volume (l×⊘)	900×306	mm^3
	volume ratio copper:sieve	5:1	m^3
boil off compensation			
	LN_2 temperature (pressure)	85 (2.2)	K (bar)
	max. cooling power	10	kW
	measured boil off rate	xx	l/s
	heat input from cryostat only. Design (measured)	600 (1100?)	W
	total heat input with recirculation. Design (measured)	1000 (1500?)	W

Table 1: Some technical specifications of the cryostat and of the cryogenic systems

3.1. The cryostat

One important conclusion of the LAGUNA-LBNO FP7 design study [2] is the technical feasibility to build giant underground cryostat up to 100 kton based on the Liquefied Natural Gas (LNG) industrial technology. The cryostats are made from corrugated stainless steel "membrane" panels that absorb the thermal stress and about 1 meter thick low density passive insulation. The study shows that it satisfies the requirement of long-term storage of ultra-pure liquid argon, and can fully accommodate a dual phase LAr TPC with the necessary cold-warm interfaces. The design studies also converged on the choice of the corrugated membrane technology licensed by GTT/France[1], which offered several advantages in the deep underground environment and for liquid argon storage (as opposed to their industrial use for LNG). A close partnership was put in place with GTT to construct the cryostat hosting the $3 \times 1 \times 1$ m^3 detector. The cryostat comes in two separate elements: the main vessel and a thermally insulated lid called top-cap under which the detector is suspended. Their thermal insulation is based on GRPF (glass reinforced polyurethane foam) layers, interspersed with pressure distributing layers of plywood. The dimensions of the cryostat are provided in Table 1 and pictures of its assembly are shown in Figure 3. The details of both elements are provided hereafter.

Figure 3: Pictures of the setup at different stages of construction. Left: the pump tower with the extractable liquid pump system. Top: the main vessel interior before and after the welding of the membrane sheets. Bottom right: the top cap with the TPC suspended during insertion in the main vessel. Bottom left: full view of the final cryostat exterior, the cryogenic system is visible on the top.

The main vessel consists of an outer structure who has a mechanical supporting role, and has to sustain the forces of the over-pressure in the inner vessel. It is a skeleton made from carbon-steel I-beams bolted together. Stainless steel plates of 6 mm thickness and 600×600 mm^2 surface are welded on its inner surface. The passive insulation comes in prefabricated panels of 330 mm thickness. Each individual panel is made of GRPF sandwiched between two sheets of Plywood. The blocks are superimposed in 3 layers in such a way to provide a uniform ~ 1 meter insulation over the entire surface. The ~ 5 cm inter spaces between

1

neighbouring insulating panels are systematically filled with sheets of fiber-glass wool to avoid convective heat transfers. Forty five temperature sensors are distributed inside the insulation space to provide feedback on the gradient and quality of the insulation during cryogenic operation. The membrane sheets come in different dimensions with various shapes of corrugations to match the geometry and thermal shrinkage calculations of the cryostat. They are fixed on the insulation panels and carefully welded together.

The top cap is a 1.2 meter thick thermal insulating lid that covers the main vessel. It is made from a top stainless steel top cover and an INVAR bottom plate. The side walls have vertical corrugations which are complementary to those from the main vessel in order to minimize the space in between the top cap and the main vessel. This gap is calculated to be 2 mm. The insulation is made from stacked sheets of GRPF; plywood panels are arranged to provide internal structural reinforcement. Altogether twenty INVAR pipes of various diameters called chimneys cross the top cap in order to host the necessary feedthroughs as well the interfaces to the cryogenic system. Each pipe is extended to the exterior by about 30 cm and terminated by a UHV flange so that the appropriate feedthrough can be fixed.

The thickness and composition of the insulation is designed to reach a residual heat input of 5 W/m^2 in cold operation. Based on those values the total heat input from the cryosat taking into account all the top-cap penetrations is estimated to be about 600 W.

Since the membrane from the main vessel and the top cap ensure the tightness and liquid containment of the cryostat under normal operating condition, all the welds are systematically inspected. Both the top cap and the main vessel have a set of external ports communicating with their insulation volumes to allow for input of gas during leak checking and to regulate the insulation space pressure during operation. Upon delivery both top-cap and main vessel are leaked checked separately by flushing Helium gas inside their respective insulation volumes and locally scanning the welds with a spectrometer. In the case of the main vessel, to increase the sensitivity of the test beyond the Helium traces present in the atmosphere ($\sim \times 10^{-5}$ mbar lt/s), custom designed vacuum plugs matching the shapes of the membrane corrugations have been developed. The plug covers about 20 cm of weld and allow to reach a vacuum better than 10^{-4} mbar in about one minute. Reaching this level of vacuum allows to check for leaks on the membrane welds down to the sensitivity limit of the spectrometer of $\sim\ 1 \times 10^{-9}$ mbar l/s. Once the top-cap and detector are inserted, the top-cap is welded to the main vessel and their insulation volumes are linked together forming one single cryosat with a common insulation. In order to remove and prevent the presence of residual humidity inside the insulation, a constant $\sim$40 liter per hour flow of gas nitrogen is introduced and exhausted through a bubbler setting the insulation volume at a $\sim$5 mbar over-pressure with respect to the atmospheric pressure.

3.2. The cryogenic and argon purification system

The principal tasks of the cryogenic and argon purification system can be summarised as follow: 1. evacuate the air from inside the cryostat to the level that its main contaminants (oxygen, moisture and nitrogen) are reduced to the part-per-million (ppm) level, 2. cool down and fill the cryostat with liquid argon in a uniform and controlled manner and 3. ensure optimal operation of the detector by setting a stable thermodynamic environment inside the cryostat while keeping the electronegative impurities in the liquid below ∼100 ppt. A detailed description of the system at each step along with its performance is provided below

3.2.1. Gas argon piston purge, cooling down and filling

In order to evacuate the air from inside the cryostat, argon gas is uniformly introduced at the bottom of the cryostat through a manifold of 4 pipes each containing three 12 mm diameter holes and is exhaust through venting pipes placed at the top of each top-cap penetrations. This "piston purge" provides a uniform gas flow from the bottom to the top of the main volume and prevents the formation of any residual air pockets. The exhaust gas from the chimney vents can either be sent to the exterior through a non-return valve or recirculated through a purifying cartridge and return to the cryostat. During the purge process, the gas impurities present inside the cryostat main volume are continuously monitored and recorded with three trace analysers for oxygen, moisture and nitrogen. The technical details of the three trace analysers are summarised in Table 2. The sample gas to the trace analysers is taken with the help of a double diaphragm pump[2] with a maximal flow capacity of 4.5 l/min. In order to compensate the gas taken by the sampling pump, a make-up gas line can inject pure argon gas through a commercial gas purifier[3]. The evolution of the impurities during the piston purge is shown in Figure 4. The process is performed in two phases. First in the so called open loop purge the input gas is injected into the cryostat with a flow rate of about 2 l/s and vented to the exterior through a non-return valve. At the end of the open loop the impurities are measured to be 0.4 ppm, 1.7 ppm and 43 ppm for oxygen, nitrogen and moisture. The comparatively larger moisture content is interpreted as stemming from the moisture attached to the surface of the cryostat, the cryogenic vessel, the process pipes and the detector components. The gas is then recirculated in closed loop by a double diaphragm pump at a flow rate of 240 l/min [4] and a commercial gas purifier [5] which filters oxygen and moisture, but has no expected effect on nitrogen. Thus, during the closed looped stage only oxygen and moisture levels decrease while nitrogen slightly rises presumably due to outgassing of the detector components inside the cryostat. The sudden increase in the nitrogen level at the beginning of the closed loop is interpreted as coming from a trapped volume of air before the gas purification cartridge. From time to time, pure argon gas is injected through the makeup gas line to dilute the nitrogen impurity, as indicated in Figure 4. At the end of the closed loop the impurities are measured to be 0.2, 3.5 and 25 ppm for oxygen, nitrogen and moisture.

The cooling down is performed by a mixture of argon gas at 300 K and LAr at 87 K which is injected through four gas atomizing nozzles [6] located at the corner of the cryostat with flow rates of 500 l/min and 21.1 l/h respectively (CHECK FIXME Caspar, you could plot the flow during the cooling down stage, this number will replace the 500 l/min). This

[2]KNF N 86 AN.12DC-B
[3]SAES MicroTorr MC400
[4]KNF 0150.1.2 AN.12 E
[5]SAES MicroTorr MC4500
[6]SSCO-Spraying Systems 1/4J-SS+SUE18-SS

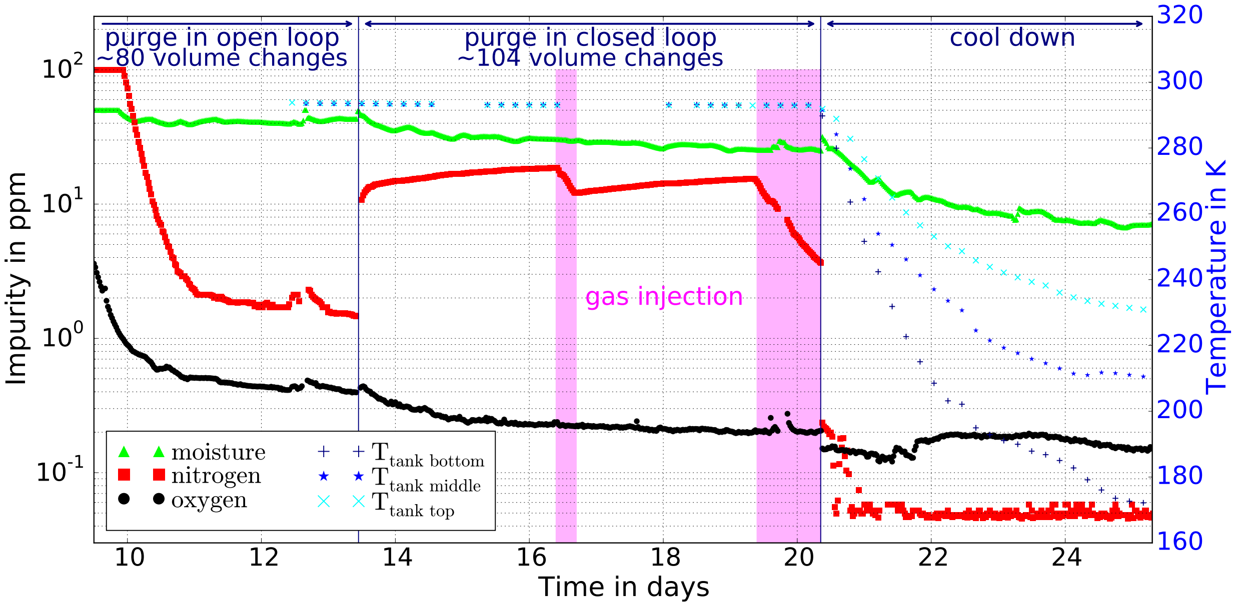

Figure 4: Evolution of the impurities measured in gas during open, closed loop piston purge and cooling down. The measured temperatures inside the gas near the bottom, middle and top of the main cryostat volume are indicated in blue.

instrument	upper detection limit	lower detection limit	precision at lowest range	provider
Oxygen	23%	50 ppb	±100 ppb	AMI (2001 R series)
Nitrogen	200 ppm	10 ppb	±0.25 ppm	Gow-mac (1200 series)
Moisture	50 ppm	10 ppb	±0.05 ppm	Gow-mac (1402 series)

Table 2: Parameters of the gas trace analysers. FIXME Shuo dicrepency between lower detection limit and precision at lowest range?

method provides a uniform and steady cooling down by generating a flat pattern of atomized argon at temperature close to 87 K. It was successfully used for the first time at FNAL in the 35 ton cryostat as reported in [13]. Various temperature probes are present in the cryostat main volume either glued on the membrane surface or fixed to the TPC, their readings are feedback to the cryogenic system to adjust the input flow of LAr and hence control the cooling power. As example we show in Figure 4, the temperature measured in the gas at 3 different heights along the detector. The cryostat is cooled down from room temperature to a minimum temperature measured on the gas of 170 K in about 5 days at an initial rate of ∼2 K per hour. The filling is then performed by... at an average rate of xx g/s (l/min)

The liquid level during filling is monitored by a chain of temperature probes evenly spaced at 4 cm spanning 1.5 meters from the bottom of the main volume to the top of the TPC drift cage. A coaxial capacitive level meter The nominal level during detector operation is set

3.2.2. Boil off compensation and liquid purification during detector operation

During detector operation the liquid is continuously recirculated and purified. A submerged centrifugal cryogenic pump[7] operating at ~20 lpm circulates the liquid through a custom built purification cartridge containing 2 separate volumes of molecular sieve[8] and copper pellets[9] to remove moisture and oxygen respectively. Some specifications of the cartridge and liquid pump are listed in Table 1. The liquid argon pump recirculates about 2 cryostat volumes per day. The unique design of the liquid pumping system is that the pump can be extracted from the tank without polluting the LAr of the main volume. The pump is confined at the bottom of a fixed vessel called pump tower which has a 350 mm diameter and a 3.5 meter length. The pump tower communicates with the main cryostat liquid and gas volume via two 25 mm diameter openings. The size of the openings can be controlled from the exterior via two long stem cryogenics valves to regulate the flow of LAr and to equalise the pressure between the pump vessel and the main volume. FIXME describe extractable part Shuo, also describe phase separator

The boil-off gas argon is continuously re-condensed by a liquid nitrogen heat exchanger. For a given heat input, the pressure inside the cryostat main volume is thus regulated by setting the flow and pressure of the liquid nitrogen. The condensed boil-off is re-injected as liquid into the pump tower where it undergoes the liquid recirculation cycle mentioned above. The liquid nitrogen heat exchanger is designed to provide compensation for up to 10 kW of heat input.

3.3. Cryostat and cryogenic system performance

During detector operation the cryostat is filled with a nominal height of 1590 mm of liquid argon. As mentioned in Section 3.1 the pressure inside the insulation volume (P_{IV}) is set at a constant $P_{IV} = P_{ATM} + 5$ mbar by flushing gas nitrogen. A gas spectrometer also continuously analyses the contents of the gas in the insulation volume in order to detect abnormal traces of argon above the average baseline which could indicate a failure of the membrane containment. Due to mechanical constraints the operating pressure of the cryostat's main volume (P_{MV}) must always remain above that of the insulation volume (P_{IV}). In addition a burst disk is set to rupture if the main volume pressure exceeds 160 mbarG. These constraints provide an upper and lower bound for the operating pressure range inside the cryostat: $P_{IS} \leq P_{MV} < P_{ATM} + 160$ mbar. From the lowest and highest atmospheric pressures recorded at CERN in the past 15 years, $930 < P_{ATM} < 990$ mbar, we set a conservative range of operation for the main volume at $995 \leq P_{MV} < 1090$ mbar. Figure 5-left shows a distribution of the recorded cryostat and atmospheric pressures during

[7]ACD TC34.2
[8]BASF 4A 8x12 mesh
[9]BASF CU 0226 S 8x14MESH

one week of data taking. As can be seen a constant 999 $\pm$ 1.4 mbar was achieved inside the main volume completely decoupled from external pressure variations. Temperature probes distributed in different places on the CRP area measure the temperature in the gas at different heights above the liquid level with a precision of about 0.1 K (see Section 6 for more details on the temperature monitoring). The measured gradient is around 2 K/cm and, as shown in Figure 5-right, the temperature measured in four points on the CRP over a one week data taking period are uniform and stable within one degree.

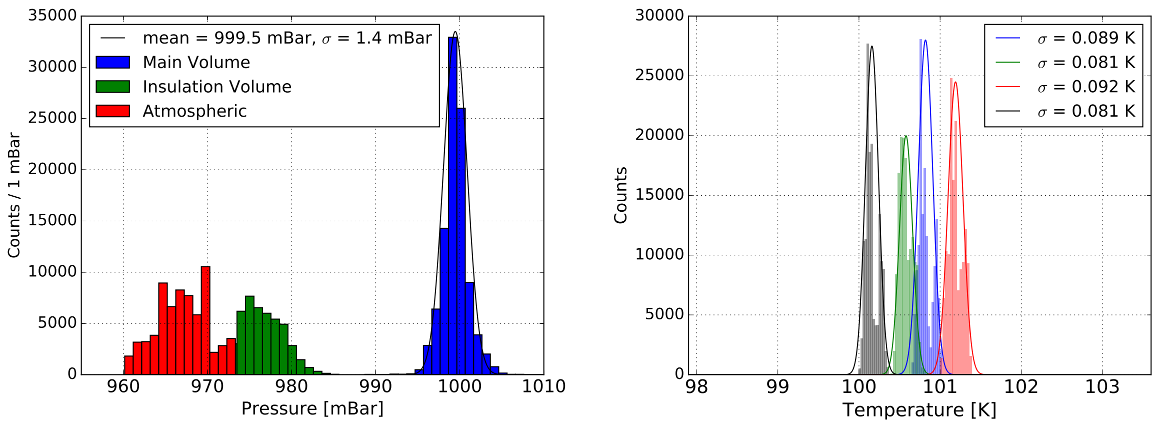

Figure 5: Pressure and temperatures measured over a one week period during data taking. Left: the pressure inside the cryosat main volume compared to that of the insulation and atmospheric. Right: the temperature measured in 4 different points on the CRP at a distance of 2.6 cm above the LEMs. The temperature and the pressure inside the tank are taken over the same period of time.

Once the cryosat is filled, the CRP motorised system together with the level meters allow to precisely position the frame to its nominal position and align it with respect to the liquid level. Both level meters and the motorised system have a precision of about 100 microns. During operation of the experiment, the cryogenic system constantly reads out the level meters to maintain a constant liquid level by adding or removing small amounts of purified liquid argon from the phase separator. This method does not introduce any large fluctuations of the liquid level which is stable within the 100 micron resolution of the level meters. This is verified in Figure 6 where the readings of the seven level meters placed on the CRP are shown for an extended period of time during data taking. All show a standard deviation at the 100 micron level, their relative offset is understood as arising from the mechanical deformations of the CRP frame in cold. More details on the frame's deformation and the alignment procedure are provided in Section 4.

The total heat input to the liquid argon arising from the cryostat and from the operation of the cryogenic system (pumps, etc..) can be estimated by measuring the rate of evaporation of the boil off gas. During operation we measured a rate of xx g/s gas, which indicates a total heat input of xxxx W, when subtracting for the heat input from the cryogenic system (mainly the liquid pump) the total estimated heat input from the cryostat only is of xxx W. These are to be compared to the design value of the cryostat insulation performance of 300

W.

The cryogenic system is thus capable to regulate the liquid argon level to a 100 micron precision while keeping a constant pressure and temperature over extended period of times. The achievements on the liquid argon purity are discussed in Section 7.

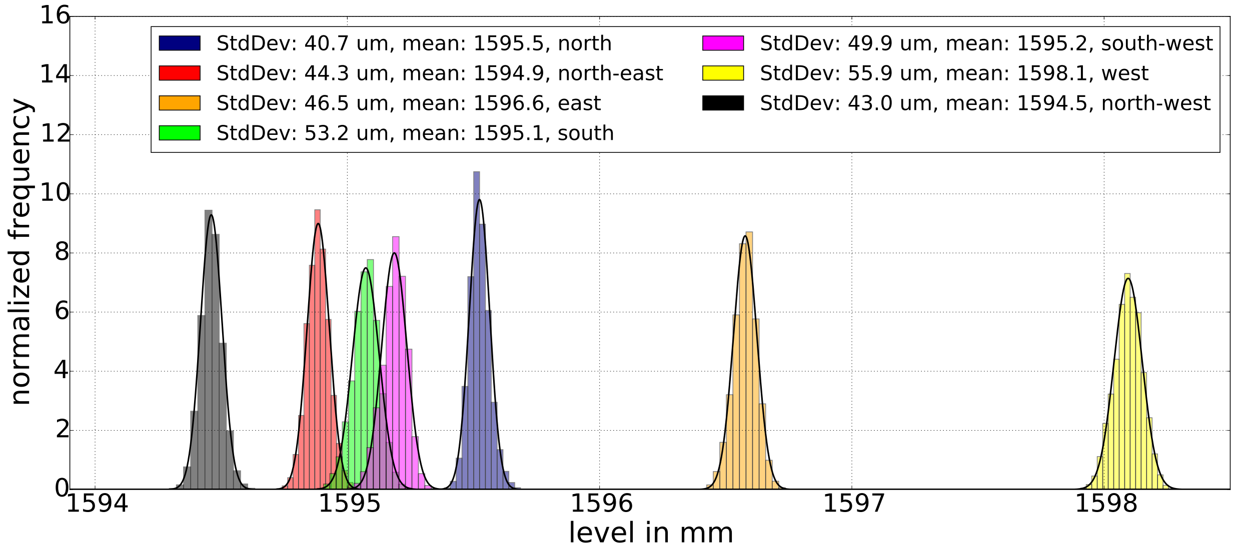

Figure 6: The level recorded by seven level meters on the CRP over a period of 6 days, fitted with normal distributions. The respective location is indicated in the legend.

4. Description of the TPC

Pictures of the $3 \times 1 \times 1$ m^3 TPC during construction and inside the cryostat

4.1. Drift cage, cathode and high voltage feedthroughs

The field cage consists of cathode and 19 identical field shaping rings placed 50 mm apart. The rings are made from a 2 mm thick stainless steel tubes 33.7 mm in diameter. The cathode plane is built from a ring (same as the field shapers) and small 4 mm diameter stainless steel pipes welded to it at the 40 mm pitch on the inside. The rings and cathode are interconnected with a pair of 100 MΩ HV-rated resistors (Metallux 969.11) forming a voltage divider chain that ensures uniform drift field inside the active TPC volume. An average increase of about 7% in the value of the resistance has been measured for these resistors at 77 K.

The resistor-divider chain is terminated to ground outside of the cryostat via an interchangeable resistor. Depending on the HV applied to the cathode, this resistor allows to set an appropriate voltage drop from the first field shaper (furthest from the cathode) to the ground as to permit electrons to continue drifting to the CRP. The entire field cage assembly is suspended from 8 FR4 pillars fastened to the top cap. The pillars also support the frame holding the 5 PMT detectors as well as a stainless steel grid (ground grid) that shields the

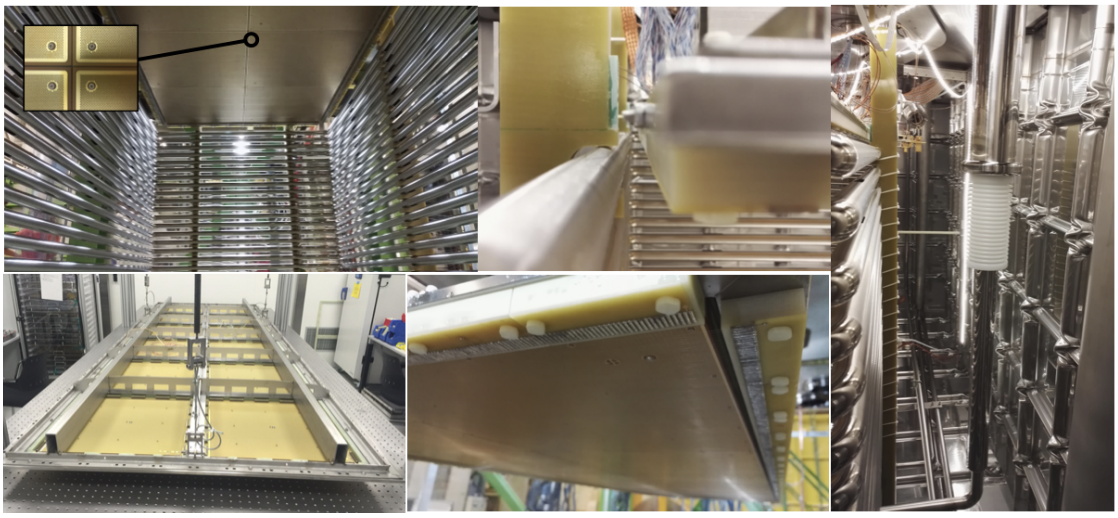

Figure 7: Some details of the TPC. Top-left picture from the drift cage interior looking up to the CRP LEM plane. Top-middle: the top of the drift cage with the CRP and first field shaping ring. Bottom: the CRP during detector assembly top and bottom view. The high voltage feedthrough connected to the cathode inside the cryostat is shown in the right picture.

latter from the cathode HV. The combined optical transparency of the cathode and ground grid is around XX%.

4.2. Charge readout plane

4.2.1. Mechanical frame and suspension system

The CRP

4.2.2. Large Area LEMs and anodes

4.2.3. LEM biasing and medium voltage feedthroughs

The 3×1 m^2 CRP is the principal element of the TPC. Its main features are illustrated in Fig. Figure 8. The ionization electrons are extracted from liquid into the vapour phase with a help of a wire grid placed 1 cm below the LEM surface. The wires are submerged in LAr nominally by 5 mm. To ensure that the electron extraction efficiency from the liquid is close to 100% , the field strength > 2 kV/cm is required [14, and references therein]. The extracted charges pass through the holes of the LEM where the high electric field (nominally $30 - 35$ kV/cm) leads to multiplication following Townsend cascades. After the LEM, electrons drift 2 mm induction gap and are collected on an anode segmented in two orthogonal views with a pitch of 3.125 mm. Optimal LEM electron transparency is achieved with induction field of 5 kV/cm. All stages (grid, LEM, anode) are assembled in the single CRP structure with precisely defined inter-stage distances and alignment. The CRP is suspended by three cables attached to stepper motors outside of the cryostat that control its orientation and position with respect to the liquid argon level. An image of the 3×1 CRP is shown in Figure 9

The LEMs are built from 1 mm thick 50×50 cm^2 Cu clad standard FR4 PCB epoxy plates. Holes of 500 μm diameter are mechanically drilled in honeycomb pattern with a

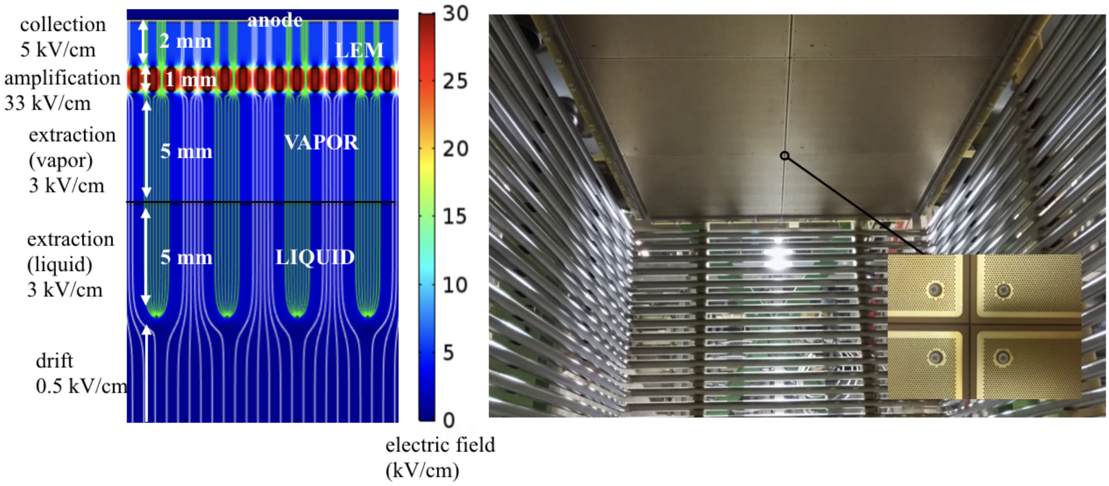

Figure 8: Illustration of the CRP region in a double phase LAr TPC. The simulated field lines in dark blue indicate those followed by the drifting charges.

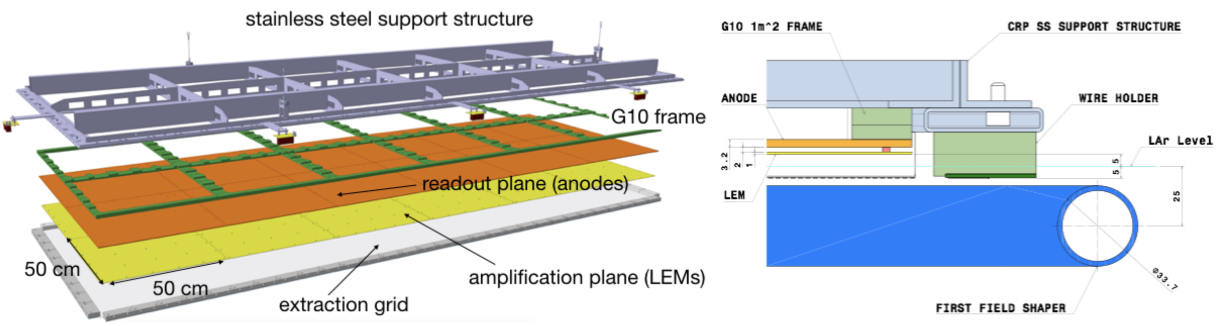

Figure 9: Exploded and cut view of the $3{\times}1$ m^2 CRP. The right plot shows in addition the nominal position of the CRP with respect to the drift cage first field shaping ring and the liquid level. Distances are shown in millimeters.

pitch of 800 μm yielding about 200 holes per cm^2. The Cu surfaces around each hole is further removed producing a 40 μm thick dielectric rim (see insert in Fig. 8). The LEM hole dimensions, pattern, and the rim size have been optimized as function of the LEM gain in [8]. Each LEM has a 4 mm border consisting of two square rings: the inner one is 2 mm wide rim from the copper cladding maintained at the same potential as the LEM surfaces and the outer is the PCB dielectric with the copper surface etched away. The function of this border is to provide protection against discharges around the edges of the LEM.

The anodes are multi-layered PCBs with an area of 50×50 cm^2 matching that of the LEMs. In the CRP the LEMs and anode are screwed into three identical $1{\times}1$ m^2 G10 frames which are then mounted on a 3×1 m^2 stainless steel structure. Each G10 support houses four LEM-anode "sandwiches" which are fixed together with insulating (peek) screws. The LEM-anode distance is ensured with a precisely machined 2 mm thick peek pillars. The distance between each adjacent LEM-anode sandwiches is 0.5 mm. Taking into account the border of each LEM gives an inactive region of 8.5 mm wide.

The extraction grid is built from 100 μm diameter stainless steel wires tensed in both x and y directions. The wire pitch of 3.125 mm matches that of the anode readout strips in order to avoid charge shadowing by the grid wires and provide a uniform extraction field. The wires are soldered on in groups of 32 on a pair of independent tensing pads. Each pad consist of a PCB fixed on a mechanical wire holder. The PCB hosts the high voltage connection and 32 soldering pads with 200 μm grooves for wire positioning. During soldering the wires had been tensed with 150 g weights. The precision on wire pitch after soldering has been verified with a microscope to be better than 50 μm. The mechanical wire holders housing the PCBs are designed to allow for the adjustment of the tension for each group of 32 wires. The holders are mounted along the outer perimeter of the CRP. Describe the weave???

TODO electrical connection of anodes figure? The anodes are interconnected with short jumper cable to form 3 m long (320 channels) and 1 m (960 channels) long readout strips in two collection views... One side is readout the other side is pulsed. The capacitance of the anode strips is an important consideration for the electronic noise of the charge amplifiers. The 2D pattern formed by the strips in the two collection views on the anode has been optimized to limit the total strip capacitance to 160 pF/m, while ensuring also that charge is evenly split between the two, independently of the azimuthal angle of particles traversing the TPC [7]. It should be noted here that this 160 pF/m capacitance of the anode is not a simple capacitance of a strip to a ground, but it rather comes from the inter-strip capacitive couplings. This fact carries some interesting implications for the noise characteristics of the readout electronics as will be discussed later.

TODO: Describe some details of HV connections on the CRP

TODO

The LEMs and anodes have been produced using industrial PCB manufacturer Eltos S.p.A. A quality assurance and control (QA/QC) procedure was established...

LEM metrology.

- LEM, anode QA
- hv connections on the CRP
- extraction grid QA manufacturing etc.. The extraction grid consists of individual pads of 32 wires tensioned across both the three meter and one meter directions. The wires are pre- tensioned and soldered on the pads one by one. Altogether we had to solder the wires on 30 pads for the 1 meter direction and 10 for the other.
- QA of CRP (bath test, photogrammetry, results)

4.3. Photon detection system

TPB coating (concentration, uniformity, QA, etc...)

The Ar scintillation light is detected with 5 cryogenic 8 inch photo-multiplier tubes (Hamamatsu R5912 - 02) placed below the ground grid underneath the cathode. The photocathode of these detectors is not sensitive to the photons below visible wavelengths and an organic wavelength shifter, tetraphenyl butadiene (TPB), is used. Three of the five PMTs were coated with TPB by evaporating it directly on the PMT glass window (concentration 0.x mg/cm^2). While for the other two, the coating was applied on transparent acrylic plates (concentration??? mg/cm^2) which were then mounted on top of the photo-detectors.

The PMT signals are acquired by an 8-channel commercial digitizer (CAEN ADC V1720) with 12 bit resolution and 250 MHz sampling rate. During the TPC operation, a time window of 1 ms — fully covering the maximal the drift time of electrons from the cathode to the anode — is read out in order to collect the light from primary (S1) and secondary (S2) scintillation. The latter is coming from the electroluminescence of electrons in the gas traversing the high E-field regions in the CRP (primarily extraction and amplification regions). The data acquisition system can be operated with an the external trigger provided by the cosmic ray trigger counters or a pulse generator (random trigger). The readout can in addition be triggered internally by setting an adjustable thresholds on all the channels in coincidence. This light-generated trigger could also be distributed to the charge-readout electronics.

5. Charge Readout scheme and data processing

5.1. Cold analog Front Ends and signal feedthrough

5.2. Front Ends cards and ASIC characteristics

5.3. Digital back end and data acquisition

6. Ancillary instrumentation and slow control

6.1. level monitoring and feedback to charge readout plane suspension

(both coax and plate) principle of operation, electronic schematics, tests, precisions,...

6.2. Cryogenic cameras

Four digital cameras capable of operating at liquid argon temperatures have been placed inside the cryostat. Their goal is essentially twofold: 1. provide visual information on the flatness and absolute level of the liquid argon and 2. check the location of potential high voltage discharges from sensitive equipments inside the tank. All cameras are identical and capable of performing both tasks, they are placed adequately in the tank based on their objectives. The image they record is shown in Figure **??**, here the cryostat is empty at room temperature. The three cameras providing the pictures *a*, *b* and *c* are fixed about 30 cm above the CRP frame in the gas argon and orientated downwards to locally verify the state of the liquid Argon level in the vicinity of the CRP level meters. As can be seen in picture *c* the entire length of the high voltage feedthrough is also captured, in particular the ground termination ring were the electric field is the highest. As discussed in [] our tests have shown that this area is is more prone to high voltage discharges. The fourth and last camera (picture *d*) is placed inside the liquid argon, it is fixed on the Photomultiplier supporting frame below the ground grid at the center of the active volume and orientated upwards capturing most of the CRP LEMs from a distance of about 1.2 meters.

The main selection criteria for the camera was its ability to undergo long term operations immersed in liquid argon while still maintaining the same image quality and without having to apply a local heat source that could induce formation of bubbles. Low power consumption, cost-effectiveness, size, and the capability to be readout at a distance of a few meters were also important aspects. A solution satisfying the above requirements was found with the commercially available Raspberry Pi[10] V1 digital camera module. Its main parameters are summarised in Table 3.

Size	25 × 24 × 9 mm
Weight	3 g
Sensor	OmniVision OV5647
Sensor resolution	2592 × 1944 pixels
Focal length	3.6 mm
Fixed focus	1 m to ∞
Focal ratio	2.9
max frame rate	120 fps
connection to Raspberry Pi computer	15 wire Flat flexible cable (FFC)
Price	25 USD

Table 3: Specifications of the Raspberry Pi digital camera module. The parameters are taken from []

Since the camera lens are not designed to match the refractive index of liquid argon immersing it directly would result in an image that is out of focus. This effect was verified multiple times: although the camera was functioning perfectly well the observed image was blurry and unusable. One alternative would be to manufacture specific lens for cameras that are placed in the liquid. The solution adopted here however consists in standardising each camera module by carefully assembling it inside a vacuum tight stainless steel casing. The casing is made from standard components and consists of a transparent DN40 CF Quartz window, a 20 mm thick spacer flange and a 15 pin SUB-D flange at the back. Special care is taken to assemble the system under argon atmosphere to avoid condensation on the lens once immersed in liquid argon.

Each camera has to be connected to its own Raspberry Pi computer through 15 wire Flat flexible cable (FFC). Lengths of up to 8 meters were tested at room and liquid argon temperature without observing image distortion. It is a 15-pin surface mounted flat flexible connector, providing two data lines, one clock lane, bidirectional control interface, 3.3 V and GND.

The cameras do not have their individual lighting, instead individually lit instead a global lighting inside the cryostat is provided by three LED strips of about 5 meters.

[10]

Although all four cameras are identical they are hence placed in strategic positions based on their use as indicated in Figure **??**

Sufficient lighting is required for the first goal

The first goal requires sufficient lighting inside the tank which is provided by LED strips of five meter length. The strips means hence can only be monitored under certain operating conditions when any light sensitive equipment is off. The second set of cameras on the contrary require a dark environment and can be operated continuously.

requires no lighting and the cameras can be left on for continuous monitoring.

when light sensitive equipment (such as PTMs) is switched off. The second

surface during filling and detector operation

The lighting inside the tank is provided by xx meters LED strips powered by 48 V DC power supplies. Points 1 and 2 require

6.3. Slow control back-end

esaily scalable SC system

7. Dector commissioning and first data

7.1. Stability of liquid level and charge readout plane adjustment

7.2. high voltage system settings and stability

7.3. Charge readout performance and response

7.3.1. Electronic noise study

7.3.2. Response to an injected pulse

3m vs 1 m strip, impedance, pulsing , signal shape etc..

7.4. Photon detection system performance

7.5. First data

7.5.1. Electroluminescence and evidence for charge extraction

7.5.2. Observation of first cosmic muons with gain

References

[1] R. Acciarri, et al., Long-Baseline Neutrino Facility (LBNF) and Deep Underground Neutrino Experiment (DUNE)arXiv:1601.02984.

[2] S. Agarwalla, et al., LAGUNA-LBNO Part 1: Liquid Argon Detectors, `http://laguna.ethz.ch:8080/Plone/deliverables/laguna-lbno-284518-deliverables` (2014).

[3] A. Bondar, A. Buzulutskov, A. Grebenuk, D. Pavlyuchenko, Y. Tikhonov, A. Breskin, Thick gem versus thin gem in two-phase argon avalanche detectors, JINST 3 (07) (2008) P07001. URL `http://stacks.iop.org/1748-0221/3/i=07/a=P07001`

[4] A. Badertscher., et al., Stable operation with gain of a double phase Liquid Argon LEM-TPC with a 1 mm thick segmented LEM, J. Phys. Conf. Ser.arXiv:1010.2482.

[5] A. Badertscher, A. Curioni, U. Degunda, L. Epprecht, A. Gendotti, et al., First operation and performance of a 200 lt double phase LAr LEM-TPC with a 40×76 cm^2 readout, JINST 8 (2013) P04012. arXiv:1301.4817, doi:10.1088/1748-0221/8/04/P04012.

[6] L. Agostino, et al., LBNO-DEMO: Large-scale neutrino detector demonstrators for phased performance assessment in view of a long-baseline oscillation experimentarXiv:1409.4405.

[7] C. Cantini, et al., Long-term operation of a double phase LAr LEM Time Projection Chamber with a simplified anode and extraction-grid design, JINST 9 (2014) P03017. arXiv:1312.6487, doi:10.1088/1748-0221/9/03/P03017.

[8] C. Cantini, et al., Performance study of the effective gain of the double phase liquid Argon LEM Time Projection Chamber, JINST 10 (03) (2015) P03017. arXiv:1412.4402, doi:10.1088/1748-0221/10/03/P03017.

[9] B. M. Gushchin, et al., Emission of hot electrons from liquid and solid argon and xenon, Sov. Phys. JETP 55(5) (1982) 860862.

[10] F. Resnati, Modeling, design and first operation of the novel double phase LAr LEM-TPC detector, Ph.D. thesis, ETH Zurich (2012).
URL http://dx.doi.org/10.3929/ethz-a-007582292

[11] A. Stahl, et al., Expression of Interest for a very long baseline neutrino oscillation experiment (LBNO).

[12] R. Acciarri, et al., Long-Baseline Neutrino Facility (LBNF) and Deep Underground Neutrino Experiment (DUNE) Conceptual Design Report, Volume 4 The DUNE Detectors at LBNFarXiv:1601.02984.

[13] A. H. B. N. J. R. R. R. J. S. D. Montanari, M. Adamowski, T. Tope, Performance and Results of the LBNE 35 Ton Membrane Cryostat Prototype, Phys. Procedia 67 (2015) 308–313.

[14] A. Bondar, A. Buzulutskov, A. Grebenuk, D. Pavlyuchenko, R. Snopkov, Y. Tikhonov, Two-phase argon and xenon avalanche detectors based on gas electron multipliers, Nucl. Instrum. Meth. A556 (2006) 273–280. arXiv:physics/0510266, doi:10.1016/j.nima.2005.10.102.